Synthesis and Characterization of the Keggin-Type Ruthenium-Nitrido Derivative [PW 11 O 39 RuN] 4- and Evidence of Its Electrophilic Reactivity

Vanina Lahootun, Claire Besson, Richard Villanneau, Françoise Villain, Lise-Marie Chamoreau, Kamal Boubekeur, Sébastien Blanchard, René Thouvenot, Anna Proust

J|A|C|S
ARTICLES
Published on Web 05/12/2007

Synthesis and Characterization of the Keggin-Type Ruthenium-Nitrido Derivative $[PW_{11}O_{39}\{RuN\}]^{4-}$ and Evidence of Its Electrophilic Reactivity

Vanina Lahootun, Claire Besson, Richard Villanneau, Françoise Villain,[§] Lise-Marie Chamoreau, Kamal Boubekeur, Sébastien Blanchard, René Thouvenot, and Anna Proust*,[†]

Contribution from the Laboratoire de Chimie Inorganique et Matériaux Moléculaires, UMR CNRS 7071, Université Pierre et Marie Curie-Paris6, Institut de Chimie Moléculaire FR2769, 4 Place Jussieu, Case 42, 75252 Paris Cedex 05, France

Received February 16, 2007; E-mail: proust@ccr.jussieu.fr

Abstract: The ruthenium-nitrido POM derivative $[PW_{11}O_{39}\{Ru^{VI}N\}]^{4-}$ has been synthesized by reaction between $[PW_{11}O_{39}]^{7-}$ and $[Ru^{VI}NCl_5]^{2-}$ or $[Ru^{VI}NCl_4]^{-}$. Its molecular structure has been confirmed from multinuclear ^{31}P and ^{183}W NMR spectroscopy together with an EXAFS study, while the oxidation state of the ruthenium bearing the nitrido ligand has been inferred both from ^{183}W NMR and XANES analysis at the Ru-K edge. The potential of $[PW_{11}O_{39}\{Ru^{VI}N\}]^{4-}$ in N-atom transfer reactions has been demonstrated through reaction with triphenylphosphine, which ultimately leads to the release of the bis(triphenylphosphane)-iminium cation $[PPh_3{=}N{=}PPh_3]^{+}$ through several intermediates, among which the phosphoraniminato derivative $[PW_{11}O_{39}\{Ru^{V}NPh_3\}]^{3-}$ has been structurally characterized. Its unusual oxidation state is in accordance with its EPR spectrum.

Introduction

Polyoxometalates (POMs) are clusters of early transition metals in their highest oxidation states bound to oxygen atoms. They form a unique class of compounds because of their structural diversity and their tunable properties.[1] They have found numerous applications in analytical chemistry, catalysis, materials science, or medicine.[2−4] In particular, many Keggin-type polyanions, incorporating one or several transition metals, have been studied for their catalytic activity in oxygenation reactions.[5−14] Their thermal stability as well as their robustness under oxidative conditions have then been put forward.[5,15,16] Although a few reports of well-described platinum-group derivatives of POMs can be found before 1990, a wider number of studies came out after the seminal publication on the characterization of the phosphotungsto-ruthenate heteropolyanions $[PW_{11}O_{39}\{RuL\}]^{n-}$ by Rong and Pope.[17,18−21] In this paper,[17] the authors showed that the porphyrin-like $[PW_{11}O_{39}]^{7-}$ ligand may be successfully used for the coordination of ruthenium cations of different oxidation states (in the range +II to +V), confirming thus that POMs are a versatile class of ligands capable of stabilizing either high or low oxidation state cations. Since then, the analogy between monovacant Keggin anions and porphyrins has also been addressed theoretically.[22] The ability of the thus-stabilized transition metal cations to

[†] Membre de l'Institut Universitaire de France.

[§] Also associated to Synchrotron SOLEIL, l'Orme des Merisiers, Saint-Aubin BP 48, 91192 Gif sur Yvette, France.

(1) Pope, M. T. *Heteropoly and Isopoly Oxometalates*; Springer-Verlag: New York, 1983.
(2) *Polyoxometalate Chemistry: From Topology via Self-Assembly to Applications*; Pope, M. T.; Müller, A., Eds., Kluwer Academic Publishers: Dordrecht, 2001.
(3) Yamase, T.; Pope, M. T., Eds. Polyoxometalate Chemistry for Nano-composite Design. In *Nanostructure Science and Technology*; Lockwood, D. J., Ed.; Kluwer Academic Publishers: New York, 2002; vol. 2.
(4) *Polyoxometalate Molecular Science*; Borras-Almenar, J. J.; Coronado, E.; Müller, A.; Pope, M. T., Eds.; Kluwer Academic Publishers: Dordrecht, 2003.
(5) Hill, C. L.; Brown, R. B. *J. Am. Chem. Soc.* **1986**, *108*, 536−538.
(6) Weinstock, I. A.; Barbuzzi, E. M. G.; Wemple, M. W.; Cowan, J. J.; Reiner, R. S.; Sonnen, D. M.; Heintz, R. A.; Bond, J. S.; Hill, C. L. *Nature* **2001**, *414*, 191−195.
(7) Okun, N. M.; Tarr, J. C.; Hilleshiem, D. A.; Zhang, L.; Hardcastle, K. I.; Hill, C. L. *J. Mol. Catal. A* **2006**, *246*, 11−17.
(8) Piepgrass, K.; Pope, M. T. *J. Am. Chem. Soc.* **1987**, *109*, 1586−1587.
(9) Neumann, R.; Abu-Gnim, C. *J. Chem. Soc., Chem. Commun.* **1989**, 1324−1325.
(10) Khenkin, A. M.; Kumar, D.; Shaik, S.; Neumann, R. *J. Am. Chem. Soc.* **2006**, *128*, 15451−15460.
(11) Lyon, D. K.; Miller, W. K.; Novet, T.; Domaille, P. J.; Evitt, E.; Johnson, D. C.; Finke, R. G. *J. Am. Chem. Soc.* **1991**, *113*, 7209−7221.
(12) Nishiyama, Y.; Nakagawa, Y.; Mizuno, N. *Angew. Chem., Int. Ed.* **2001**, *40*, 3639−3641.
(13) Botar, B.; Geletii, Y. V.; Kogerler, P.; Musaev, D. G.; Morokuma, K.; Weinstock, I. A.; Hill, C. L. *J. Am. Chem. Soc.* **2006**, *128*, 11268−11277.
(14) Bonchio, M.; Carraro, M.; Sartorel, A.; Scorrano, G.; Kortz, U. *J. Mol. Catal. A* **2006**, *251*, 93−99.
(15) Hill, C. L.; Prosser-McCartha, C. M. *Coord. Chem. Rev.* **1995**, *143*, 407−455.
(16) Mizuno, N.; Misono, M. *Chem. Rev.* **1998**, *98*, 199−218.
(17) Rong, C.; Pope, M. T. *J. Am. Chem. Soc.* **1992**, *114*, 2932−2938.
(18) Neumann, R.; Khenkin, A. M.; Dahan, M. *Angew. Chem., Int. Ed. Engl.* **1995**, *34*, 1587−1589.
(19) Neumann, R.; Dahan, M. *Nature* **1997**, *388*, 353−355.
(20) Anderson, T. M.; Neiwert, W. A.; Kirk, M. L.; Piccoli, P. M. B.; Schultz, A. J.; Koetzle, T. F.; Musaev, D. G.; Morokuma, K.; Cao, R.; Hill, C. L. *Science* **2004**, *306*, 2074−2077.
(21) Anderson, T. M.; Cao, R.; Slonkina, E.; Hedman, B.; Hodgson, K. O.; Hardcastle, K. I.; Neiwert, W. A.; Wu, S. X.; Kirk, M. L.; Knottenbelt, S.; Depperman, E. C.; Keita, B.; Nadjo, L.; Musaev, D. G.; Morokuma, K.; Hill, C. L. *J. Am. Chem. Soc.* **2005**, *127*, 11948−11949.
(22) Visser, S. P.; Kumar, D.; Neumann, R.; Shaikh, S. *Angew. Chem., Int. Ed.* **2004**, *43*, 5661−5665.

transfer oxygen atom being well established, it seemed interesting to us to explore the nitrogen donor ability of nitrido derivatives of Keggin-type POMs, on which we are now focusing our attention, as part of our general program on nitrogenous derivatives of POMs.[23−27] However, up to date, very few metal-nitrido derivatives of polyanions have been synthesized.[28,29] We have recently reported the osmium- and rhenium-nitrido derivatives of the Keggin- and Dawson-type anions: $[PW_{11}O_{39}\{OsN\}]^{4-}$, α_1- and α_2-$[P_2W_{17}O_{61}\{OsN\}]^{7-}$, and $[PW_{11}O_{39}\{ReN\}]^{n-}$ (n = 4 or 3, for $Re^{VI}N$ and $Re^{VII}N$, respectively),[30−31] the reactivity of the latter being up to now disappointing. Recently, examples of alkene amination and aziridination by ruthenium-nitrido porphyrin and ruthenium-nitrido salen complexes have been reported.[32,33] These illustrate the versatility of the reactivity of the ruthenium-nitrido function from electrophilic, in the direct aziridination of alkenes,[32] to nucleophilic, with prior activation by trifluoroacetic anhydride.[33] The possibility to tune the reactivity of the ruthenium-nitrido function by playing with the ligand or the oxidation state of the metal prompted us to study the synthesis of ruthenium-nitrido derivatives of Keggin-type POMs. We thus describe here the synthesis and full characterization of $[PW_{11}O_{39}\{Ru^{VI}N\}]^{4-}$, which has been isolated as cesium or *n*-tetrabutylammonium (TBA) salts. The nitrido derivative was obtained by direct reaction of $K_7[PW_{11}O_{39}]$ with a ruthenium-nitrido precursor, either $Cs_2[RuNCl_5]$ or $TBA[RuNCl_4]$. We also report herein that $[PW_{11}O_{39}\{RuN\}]^{4-}$ contains an electrophilic nitrogen atom, which reacts with phosphines.

Results and Discussion

Synthesis and Stability of $[PW_{11}O_{39}\{Ru^{VI}N\}]^{4-}$ (1) in Water. Cesium and rubidium salts of $[PW_{11}O_{39}\{Ru^{VI}N\}]^{4-}$ were synthesized by direct reaction of $K_7[PW_{11}O_{39}]$ with $Cs_2[Ru^{VI}NCl_5]$ or $Rb_2[Ru^{VI}NCl_5]$ in water. This reaction resulted in the immediate precipitation of the cesium (Cs-**1**) or rubidium (Rb-**1**) salt as a greyish-green solid, in a fairly good yield. However, because compounds Cs-**1** and Rb-**1** are insoluble in all solvents (including water), their characterization in solution was rendered impossible. In the case of Cs-**1**, its purity was ascertained by ^{31}P MAS NMR, since only one isotropic signal was observed at −14.5 ppm, and by EDX spectroscopy (ratio W:Ru identical to the previously characterized ruthenium derivative of the $[PW_{11}O_{39}]^{7-}$ anion, $Cs_5[PW_{11}O_{39}\{Ru(p\text{-cymene})(H_2O)\}]$,[34] see Supporting Information). The reaction

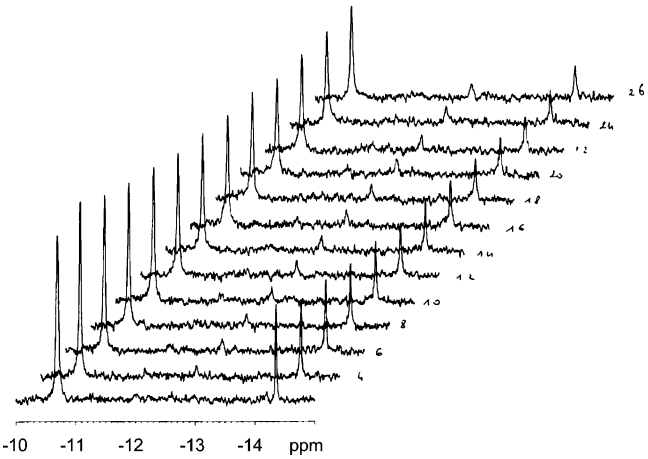

Figure 1. ^{31}P NMR monitoring of the reaction of $K_7[PW_{11}O_{39}]$ with $K_2[RuNCl_5]$ in aqueous solution (spectra recorded every 35 mn) at the concentration of 5×10^{-2} mol L^{-1}

of $[PW_{11}O_{39}]^{7-}$ with an equimolar amount of $K_2[Ru^{VI}NCl_5]$ was followed by ^{31}P NMR spectroscopy at regular intervals of time. In this case, no precipitation occurred, and the ^{31}P NMR spectrum of the mother solution, recorded after 15 min, displayed two signals with a relative intensity of 3:1 at −10.6 ppm and −14.4 ppm, corresponding to $[PW_{11}O_{39}]^{7-}$, and most probably to the functionalized polyanion $[PW_{11}O_{39}\{Ru^{VI}N\}]^{4-}$ (**1**), respectively. The chemical shift of the latter signal, as well as that observed in the solid-state above, is indeed characteristic of a refilled polyanion, (see below the ^{31}P NMR spectrum of **TBA-1** and the IR spectra of **Cs-1** and **TBA-1**). The ^{31}P NMR spectra obtained after every 35 min are represented in Figure 1. These spectra clearly illustrate that while **1** is formed almost immediately, it is rather unstable in aqueous solution and is progressively converted to a third, yet unidentified, species, characterized by a signal at −12.7 ppm. Moreover, the $[PW_{11}O_{39}]^{7-}$ anion remains the major species in solution in this case.[35] These results thus prompted us to investigate the synthesis of the ruthenium-nitrido POM in organic solvents in order to increase the yield of the reaction and to avoid the evolution of the product.

Synthesis of $TBA_4[PW_{11}O_{39}\{Ru^{VI}N\}]$ (TBA-1). While the synthesis of $TBA_4[PW_{11}O_{39}\{Re^{VI}N\}]$ has been achieved by the reaction of $TBA_4[H_3PW_{11}O_{39}]$ with $TBA[Re^{VI}NCl_4]$ in acetonitrile and in the presence of triethylamine,[30] no reaction was observed between $TBA_4[H_3PW_{11}O_{39}]$ and $TBA[Ru^{VI}NCl_4]$ even after 4 days, be it at room temperature or under reflux. This lack of reactivity is surprising since ligand substitution on $[RuNCl_4]^-$ is known to be easy and has previously been reported in the literature.[36] Considering the reactivity observed in water, we thus turned to a mixed organic/water medium: $K_7[PW_{11}O_{39}]$ was reacted with an equimolar amount of $TBA[Ru^{VI}NCl_4]$ in a H_2O/CH_3CN mixture so as to produce $TBA_4[PW_{11}O_{39}\{Ru^{VI}N\}]$ (**TBA-1**) as a green precipitate, which could be recrystallized from acetonitrile. Its ^{31}P NMR spectrum, recorded in CD_3CN at room temperature, is characterized by a signal at −13.8 ppm. Adventitious contamination by $[PW_{11}O_{39}]^{7-}$ or $[PW_{12}O_{40}]^{3-}$ could be checked at −12.0 ppm and −14.1 ppm, respectively.

(23) Proust, A.; Thouvenot, R.; Robert, F.; Gouzerh, P. *Inorg. Chem.* **1993**, *32*, 5299−5304.
(24) Proust, A.; Thouvenot, R.; Chaussade, M.; Robert, F.; Gouzerh, P. *Inorg. Chim. Acta* **1994**, *224*, 81−95.
(25) Bustos, C.; Hasenknopf, B.; Thouvenot, R.; Vaissermann, J.; Proust, A.; Gouzerh, P. *Eur. J. Inorg. Chem.* **2003**, 2757−2766.
(26) Dablemont, C.; Proust, A.; Thouvenot, R.; Afonso, C.; Fournier, F.; Tabet, J. C. *Inorg. Chem.* **2004**, *43*, 3514−3520.
(27) Dablemont, C.; Proust, A.; Thouvenot, R.; Afonso, C.; Fournier, F.; Tabet, J. C. *Dalton Trans.* **2005**, 1831−1841.
(28) Kang, H.; Zubieta, J. *J. Chem. Soc., Chem. Commun.* **1988**, 1192−1193.
(29) Abrams, M. J.; Costello, C. E.; Shaikh, S. N.; Zubieta, J. *Inorg. Chim. Acta* **1991**, *180*, 9−11.
(30) Kwen, H.; Tomlinson, S.; Maatta, E. A.; Dablemont, C.; Thouvenot, R.; Proust, A.; Gouzerh, P. *Chem. Commun.* **2002**, 2970−2971.
(31) Dablemont, C.; Hamaker, C. G.; Thouvenot, R.; Sojka, Z.; Che, M.; Maatta, E. A.; Proust, A. *Chem. Eur J.* **2006**, *12*, 9150−9160.
(32) Man, W.-L.; Lam, W. W. Y.; Yiu, S.-M.; Lau, T.-C.; Peng, S.-M. *J. Am. Chem. Soc.* **2004**, *126*, 15336−15337.
(33) Leung, S. K.-Y.; Huang, J.-S.; Liang, J.-L.; Che, C.-M.; Zhou, Z.-Y. *Angew. Chem., Int. Ed.* **2003**, *42*, 340−343.
(34) Artero, V.; Laurencin, D.; Villanneau, R.; Thouvenot, R.; Herson, P.; Gouzerh, P.; Proust, A. *Inorg. Chem.* **2005**, *44*, 2826−2835.
(35) After 24 h, the ^{31}P NMR spectrum of the solution no longer showed any signal at −14.4 ppm. In a similar manner the IR spectrum showed the disappearance of the band at 1072 cm^{-1}.
(36) Chan, P.-M.; Yu, W.-Y.; Che, C.-M.; Cheung, K.-K. *J. Chem. Soc. Dalton Trans.* **1998**, 3183−3190.

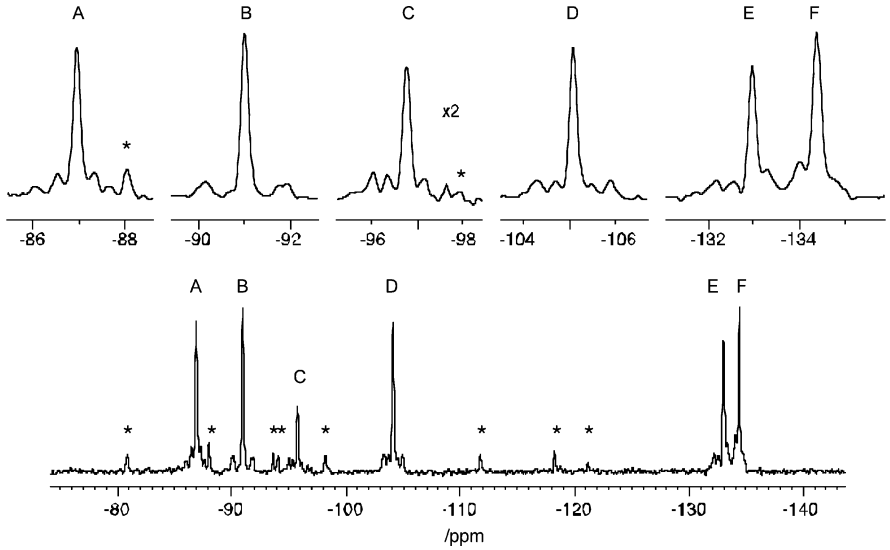

Figure 2. $^{183}W\{^{31}P\}$ NMR spectrum (12.5 MHz) of $TBA_4[PW_{11}O_{39}\{Ru^{VI}N\}]$ (**TBA-1**) (1.2×10^{-1} mol.L^{-1} in DMF/d_6-acetone ($T = 262$ K). Bottom: full spectrum; top: abscissa expansion of the individual resonances. The signal marked by * correspond to $[H_nPW_{11}O_{39}]^{(7-n)-}$ (ca 15%) and to $[PW_{12}O_{40}]^{3-}$ (ca. 2%) impurities.

The ratio of acetonitrile to water in the solvent mixture used for the reaction, which is a compromise between solubility and reactivity, as well as the duration of the stirring, has been improved to maximize product, in the highest purity. However, the overall yield remains low, 32% based on the limiting TBA, and only 8% based on Ru. Attempts to increase the yield by adding TBABr resulted in the precipitation of less pure samples. After filtration of **TBA-1**, the ^{31}P NMR spectrum of the mother liquor displayed almost no signal that can be attributed to $[PW_{11}O_{39}]^{7-}$ or to $[PW_{11}O_{39}\{Ru^{VI}N\}]^{4-}$, but rather several extra peaks of unidentified compounds. This demonstrates that (i) it is indeed not worth adding TBABr to increase the yield in **TBA-1**, and (ii) it is not worth adding an excess of $TBA[Ru^{VI}NCl_4]$, since all the $[PW_{11}O_{39}]^{7-}$ has already been transformed. Once separated from the mother liquor, **TBA-1** is stable in acetonitrile solution for several days, as checked by ^{31}P NMR.

Structural Characterization of $TBA_4[PW_{11}O_{39}\{Ru^{VI}N\}]$ (TBA-1). IR Spectroscopy. The infrared spectrum of **TBA-1** (see Supporting Information) shows as expected the characteristic features of a Keggin-type structure with strong vibrational bands at 811 cm^{-1}, 889 cm^{-1}, and 962 cm^{-1} corresponding to ν(W−O−W) and ν(W═O$_t$) stretching frequencies. The incorporation of the {RuN} function in the lacunary $[PW_{11}O_{39}]^{7-}$ restores partially a pseudo-tetrahedral geometry for **1**. This is clearly seen by the relatively low splitting of the ν(P═O) stretching mode in $[PW_{11}O_{39}\{Ru^{VI}N\}]^{4-}$ ($\Delta\bar{\nu}$ ca. 20 cm^{-1}) by comparison with the lacunary one ($\Delta\bar{\nu}$ 45 cm^{-1}).[37−39] The residual splitting observed in **1** arises most likely from the smaller size of Ru^{6+} ($r = 53$ pm) with respect to W^{6+} ($r = 60$ pm); the ruthenium cation is not able to completely refill the lacuna and to interact efficiently with the oxygen atom of the central PO_4 unit. The presence of the RuN bond cannot be ascertained by IR spectroscopy because its stretching mode is expected around 1050 cm^{-1} as a weak band, which is eventually hidden by the strong ν(P═O) band at 1072 cm^{-1}.[32,33,40]

^{183}W NMR. The relatively high solubility of **TBA-1** in dimethylformamide gives ^{183}W NMR spectra with good signal/noise ratio as required to observe tungsten−tungsten satellites. The 0.12 mol L^{-1} DMF solution spectrum of **TBA-1** obtained at 262 K (−11 °C) exhibits six major lines A, B, C, D, E, and F at −86.9 (2W), −91.0 (2W), −95.7 (1W), −104.1 (2W), −133.0 (2W), and −134.4 (2W) ppm. Minor signals are also present at −80.8, −88.0, −93.6, −94.1, −98.2, −111.8, and −118.2 ppm, which correspond to less than 15% (from ^{31}P NMR) of the lacunary Keggin anion $[H_nPW_{11}O_{39}]^{(7-n)-}$ and to residual amount (less than 2% of $[PW_{12}O_{40}]^{3-}$) (Figure 2 bottom). The ^{183}W NMR spectrum of **1** fully agrees with the C_s symmetry of a monosubstituted Keggin anion.[30,31,41−43] Moreover the narrow δ range (less than 50 ppm), without any strongly shifted resonance, is consistent with a diamagnetic compound. While many ruthenium derivatives of POMs have been reported to be paramagnetic, there are relatively few diamagnetic Ru-substituted Keggin compounds which were investigated by ^{183}W NMR: the diamagnetic anions $[PW_{11}O_{39}\{Ru^{II}L\}]^{5-}$ reported until now display strongly positively shifted signals assigned to the tungsten nuclei in the neighbor of the d^6 Ru metal. (L = H_2O, $\delta = 292.8$ and 159.3 ppm;[17] L = DMSO, $\delta = 117.4$ and −2.7 ppm).[44] Although it is unlikely that a ruthenium atom bearing a nitrido ligand could be a Ru^{2+}, the question of its oxidation state has to be addressed owing to the wide range of available oxidation states for Ru and the many examples of redox processes occurring during the synthesis of Ru derivatives. ^{183}W NMR seems to be able to answer this question; actually the ^{183}W NMR spectrum of **1** is reminiscent of that of $[PW_{11}O_{39}\{Os^{VI}N\}]^{4-}$ while it deviates markedly from those of $[PW_{11}O_{39}\{Ru^{II}L\}]^{5-}$ by the absence of any positively shifted signal. It appears then more likely that the ruthenium

(37) Rocchiccioli-Deltcheff, C.; Thouvenot, R. *J. Chem. Res. (S)* **1977**, 46−47.
(38) Rocchiccioli-Deltcheff, C.; Thouvenot, R. *J. Chem. Res. (M)* **1977**, 549−571.
(39) Peacock, R. D.; Weakley, T. J. R. *J. Chem. Soc. (A)* **1971**, 1937.
(40) Griffith, W. P.; Pawson, D. *J. Chem. Soc., Dalton Trans.* **1973**, *5*, 1315−1320.
(41) Brévard, C.; Schimpf, R.; Tourné, G.; Tourné, C. M. *J. Am. Chem. Soc.* **1983**, *105*, 7059−7063.
(42) Domaille, P. J. *J. Am. Chem. Soc.* **1984**, *106*, 7677−7687.
(43) Proust, A.; Fournier, M.; Thouvenot, R.; Gouzerh, P. *Inorg. Chim. Acta* **1994**, *215*, 61−66.
(44) Bagno, A.; Bonchio, M.; Sartorel, A.; Scorrano, G. *Eur. J. Inorg. Chem.* **2000**, 17−20.

Table 1. Experimental Tungsten−Tungsten Connectivity Matrix for [α-$PW_{11}O_{39}\{Ru^{VI}N\}]^{4-}$ (at 262 K) and in Brackets for [α-$PW_{11}O_{39}\{Os^{VI}N\}]^{4-}$ (at 300 K): On-diagonal Terms, Chemical Shifts (in ppm); Off-diagonal Terms, Coupling Constants (in hertz)

nucleus	line	2,3	4,9	5,8	6,7	10,12	11
2,3	F	−134.4		≈10	≈10		
		(−216.6)		(10.6)	(10.6)		
4,9	B		−91.0	≈23		≈20 (AB)	
			(−148.3)	(23.5)		(20.2)	
5,8	E	≈10	>20	−133.0	≈10	??	
		(11.2)	(23.5)	(−146.4)	(11.2)	(21)	
6,7	A	≈10		≈ 10	−86.9		20.6 AB
		(10.6)		(10.6)	(−84.7)		(20.8)
10,12	D		≈20	≈20		−104.1	9.8
			(20.5)	(20.5)		(−100.2)	(10)
11	C				20.4 AB	9.8	−95.7
					(20.5)	(10)	(−99.5)

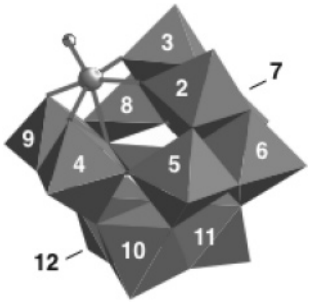

Figure 3. Postulated structure of $[PW_{11}O_{39}\{Ru^{VI}N\}]^{4-}$ with W labels according to IUPAC convention.

atom retains a d^2 configuration (Ru^{VI}) during the synthesis of **1**. The great similarity between the ^{183}W spectra of $[PW_{11}O_{39}\{Os^{VI}N\}]^{4-}$ and $[PW_{11}O_{39}\{Ru^{VI}N\}]^{4-}$ is beneficial to assign the resonances of the latter, by comparison with the former.

The strategy for the assignment is based upon the observation and quantification of W−W satellites[45] and is developed in the Supporting Information. The attribution to the W atoms labeled as in Figure 3 is displayed in Table 1, along with that of $[PW_{11}O_{39}\{Os^{VI}N\}]^{4-}$ for comparison.

Both Ru and Os nitrido derivatives present some common features:

First, all $^2J_{W-W}$ coupling constants are in the "classical" range for a saturated Keggin anion, that is ca. 10 Hz for edge coupling and ca. 20 Hz for corner coupling (except for $J_{W4-W5} \equiv J_{W8-W9}$ ca. 23 Hz for the two anions), which means that both Ru^{VI} and Os^{VI} are of appropriate size to interact with all oxygen atoms bordering the lacuna and therefore to restore practically the regular geometry of the tungsten framework.[46]

Second, the resonances of the Ws remote from the {MN} (M = Ru or Os) function have nearly the same chemical shifts in both anions.

Third, the most shielded Ws remain those corner-connected to M, i.e., W2≡W3.[48]

However, the two POM-nitrido species differ markedly by the shielding of both tungsten nuclei in the close vicinity of the $\{M^{VI}N\}$ function: by comparison with $[PW_{11}O_{39}\{Os^{VI}N\}]^{4-}$ these W nuclei are significantly deshielded in the ruthenium derivative **1** by more than 80 ppm for W2≡W3 and nearly 60 ppm for W4≡W9. The more remote nuclei W5≡W8, adjacent to the previous one's nuclei, are also deshielded, while to a lesser extent (ca + 15 ppm).

The origin of the deshielding (i.e., paramagnetic shift) experienced by W nuclei close to d^6 addenda atoms in diamagnetic $[PW_{11}O_{39}\{ML\}]^{x-}$ has been discussed by Rong and Pope and may be accounted for by a delocalization of the d-electrons from the metal to the POM framework.[17] The extent of this delocalization and consequently the amplitude of the paramagnetic shift depend on the electron density in the HOMO and on the donor−acceptor ability of the ligand L. For the POM nitrido species the corresponding W nuclei experience opposite (i.e., diamagnetic) shifts, which may be due to the different symmetry properties of the HOMO of the d^2 metal centers; the difference observed between Os and Ru is likely due to a better delocalization of the electronic density for Os (difference of energy levels of HOMOs).

XAS Measurements. Solid-state absorption spectra were recorded at room temperature for **TBA-1** and **Cs-1** so as to confirm the oxidation state of the incorporated Ru and the structure of the formed polyanion. The spectra of both compounds are clearly superimposable (see Supporting Information). The conclusions arising from the study of **TBA-1** are then valid for **Cs-1**. Figure 4 shows the Ru-K X-ray absorption near-edge spectra for reference compounds containing ruthenium in different valence states (Ru^0, $[Ru^{III}(acac)_3]$ (acac = acetylacetonate), $[Ru^{IV}O_2]$, and [(salchda)Ru^{VI}N](ClO_4), (salchda = *N*,*N*′-bis(salicylidene)*o*-cyclohexyldiamine dianion)[32] as well as that of compound **TBA-1**.[49] As expected, the position of the absorption edge is dependent on the oxidation state of the ruthenium; the higher the oxidation state the higher its energy. As the absorption edge of compound **TBA-1** is close to that of [(salchda)Ru^{VI}N](ClO_4), and lies higher in energy, it strongly suggests a +VI oxidation state for the ruthenium center in the polyanion, in accordance with the NMR data.

Also interestingly, compound **TBA-1** and [(salchda)Ru^{VI}N]-(ClO_4) both exhibit in the Ru-K near-edge absorption spectra according to the inset of Figure 4, the shoulder might be pointed at ca. 22120 eV instead of 22124 eV. In a general way, this part of the spectrum is very sensitive to the local symmetry

(45) Agustin, D.; Dallery, J.; Coelho, C.; Proust, A.; Thouvenot, R. *J. Organomet. Chem.* **2007**, *692*, 746−754.
(46) Note this is not the case for the larger Ru^{II} cation which cannot enter the cavity: Bagno *et al*. have measured corner couplings ranging from 16.1 to 26.2 Hz in $[PW_{11}O_{39}\{Ru^{II}DMSO\}]^{5-}$; these values are closer to that of the lacunary anion $[PW_{11}O_{39}]^{7-}$ (see ref 44).
(47) Cadot, E.; Thouvenot, R.; Tezé, A.; Hervé, G. *Inorg. Chem.* **1992**, *31*, 4128−4133.
(48) It should be noted however that because of different temperature coefficients, at a higher temperature, specifically 333 K (60 °C), W5≡W8 becomes the most shielded.
(49) Note that [(salchda)Ru^{VI}N](ClO_4) was preferred to TBA[$Ru^{VI}NCl_4$] as a reference compound because the nature of its coordinated atoms, N and O, rather than Cl, are closer to the nature of the coordination sphere in **TBA-1**.

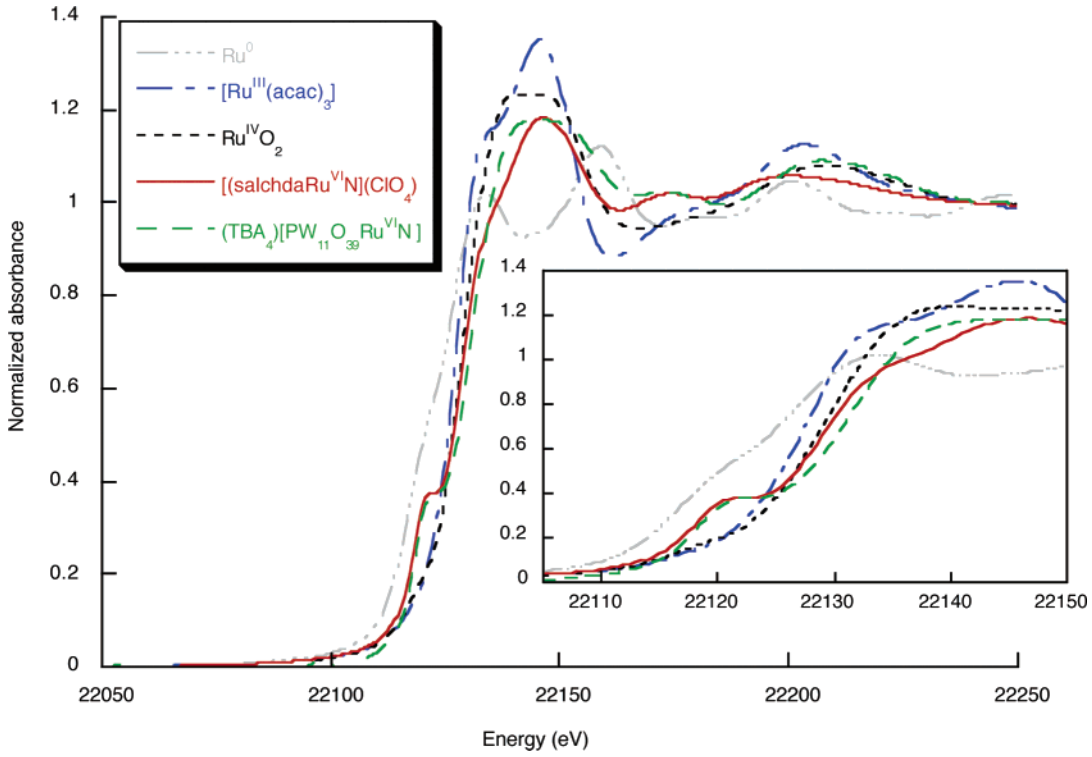

Figure 4. Ru-K edge XANES spectra of Ru^0 (in gray), $[Ru^{III}(acac)_3]$ (in blue), $Ru^{IV}O_2$ (in black), [(salchda)RuN](ClO_4) (in red), and $TBA_4[PW_{11}O_{39}\{Ru^{VI}N\}]$ (**TBA-1**) (in green).

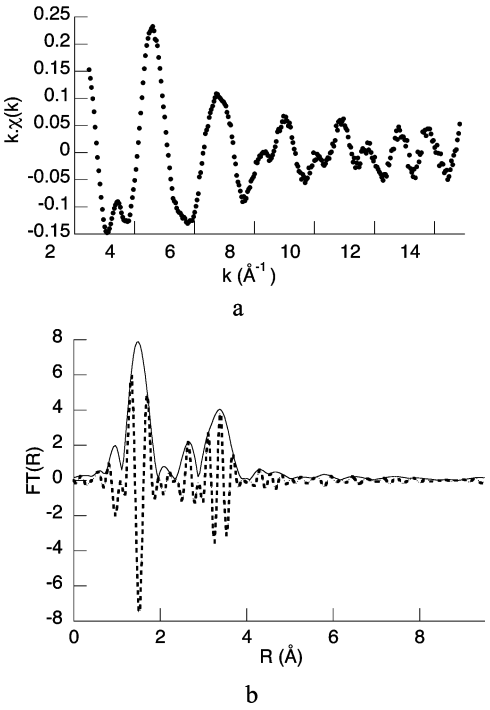

Figure 5. (a) Ru-K edge EXAFS signal and (b) the corresponding Fourier transform (modulus and imaginary part) of $TBA_4[PW_{11}O_{39}\{Ru^{VI}N\}]$ (**TBA-1**).

around the cation. The observation of such shoulders is well documented for transition-metal cations.[50,51] They are almost independent of the electronic state of the metal but are due to

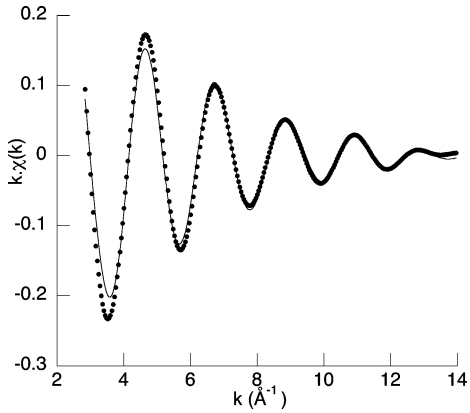

Figure 6. Filter (between 1 and 2.5 Å) of the Ru-K edge EXAFS signal of **TBA-1** (experimental data in dotted line and simulated data as the straight line).

the lowering of the local symmetry. In our particular case, this lowering of symmetry is directly related to the presence of the very short metal-nitrido bond, as systematically observed for other metal-nitrido-containing compounds.[52,53]

The geometric parameters around the ruthenium atom in **TBA-1** were then obtained from the extended X-ray absorption fine structure (EXAFS) study of this compound (Figure 5). Many metallic derivatives of the $[XW_{11}O_{39}]^{n-}$ anions have been described in the literature. In a general way, the $[XW_{11}O_{39}]^{n-}$ anion may be considered as a tetradentate or a pentadentate ligand, depending on the nature of the cation incorporated into the structure. For instance, the polyanion behaves as a tetradentate ligand in $[Ce\{PW_{11}O_{39}\}_2]^{10-}$,[54] but as a pentadentate ligand

(50) Benzekri, A.; Cartier dit Moulin, C.; Latour, J.-M.; Limosin, D.; Rey, P.; Verdaguer, M. *Inorg. Chim. Acta* **1996**, *252/1−2*, 413−420.
(51) Okamoto, K.; Miyawaki, J.; Nagai, K.; Matsumura, D.; Nojima, A.; Yokoyama, T.; Kondoh, H.; Ohta, T. *Inorg. Chem.* **2003**, *42*, 8682−8689.
(52) Niewa, R.; Hu, Z.; Kniep, R. *Eur. J. Inorg. Chem.* **2003**, 1632−1634.
(53) Laplaza, C. E.; Johnson, M. J. A.; Peters, J. C.; Odom, A. L.; Kim, E.; Cummins, C. C.; George, G. N.; Pickering, I. J. *J. Am. Chem. Soc.* **1996**, *118*, 8623−8638.

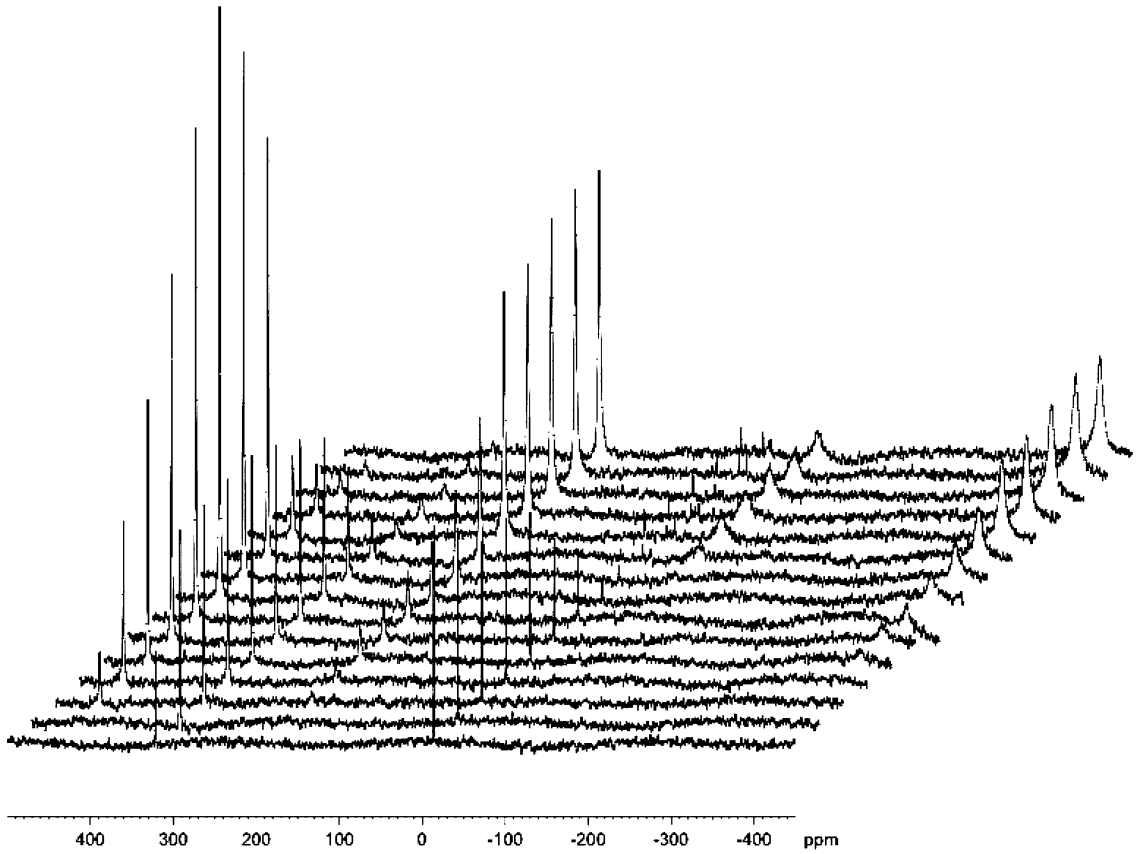

Figure 7. ^{31}P NMR spectrum of $TBA_4[PW_{11}O_{39}\{Ru^{VI}N\}]$ (**TBA-1**) in CH_3CN/CD_3CN (3:1) in the presence of increasing amounts (from 0.1 (bottom) to 2.9 (top) equiv) of triphenylphosphine.

in $[SiW_{11}O_{39}\{Ru^{III}(dmso)\}]^{5-}$(DMSO = dimethyl sulfoxide),[55] with four Ru−O distances in the range 1,90−2,01 Å and a longer one at about 2.14 Å.

As in the latter example, $[PW_{11}O_{39}]^{7-}$ may be considered as a pentadentate ligand in compound **TBA-1**. Figure 6 shows the experimental and simulated filter (between 1 and 2.5 Å) of the EXAFS signal for **TBA-1**. The corresponding modulus and imaginary part of the Fourier transform are given in the Supporting Information. Because the simulated FT of the spectrum is in close agreement with the experimental data, the peaks can be unambiguously assigned. As expected, three different distances were observed around the Ru cation corresponding to four Ru−O bonds at 1.97 Å, one Ru−O bond at 2.53 Å, with the tetrahedral PO_4^{3-} unit, and a short Ru−N triple bond at 1.67 Å, which is in good agreement with the reported ruthenium-nitrido distances ranging from 1.592(4)[32] to 1.656-(5)[33] Å determined by X-ray crystallography.

Reactivity of $TBA_4[PW_{11}O_{39}\{Ru^{VI}N\}]$ (TBA-1). In a first attempt to study its ability in nitrogen-atom transfer, **TBA-1** was reacted with cyclohexene in the presence of trifluoroacetic anhydride, at low temperature. No reaction at all was observed in this case, suggesting **TBA-1** to be poorly reactive toward electrophiles. This lack of reactivity might be due to the electron-withdrawing properties of the POM causing the nitrogen atom to be electrophilic rather than nucleophilic. Indeed ruthenium-nitrido complexes are expected to be more electrophilic than the corresponding osmium-nitrido complexes, whose reactivity can be finely tuned by the ancillary ligands from nucleophilic to electrophilic.[56] We therefore investigated the reactivity of **TBA-1** with phosphines.

Hence, the reaction of $TBA_4[PW_{11}O_{39}\{Ru^{VI}N\}]$ with increasing amounts of triphenylphosphine was monitored by ^{31}P NMR (Figure 7, see Supporting Information for an extension in the +30−15 ppm region) in a 3:1 mixture of CH_3CN:CD_3CN. For small amounts of phosphine added (less than half an equivalent), ^{31}P NMR indicates the formation of only one species **2**, characterized by a signal at 322 ppm ($\Delta\nu_{1/2}$ = 90 Hz). Compound **2** was separated from unreacted **TBA-1** by silica column chromatography and recrystallized from acetonitrile/ether. A preliminary single crystal analysis of **2** proved it to be the phosphoraniminato derivative $TBA_3[PW_{11}O_{39}\{Ru^{V}NPPh_3\}]$. Unfortunately, the poor quality of the crystals, which showed decomposition even when placed in the mother liquor in a sealed tube, and some disorder encountered within the phenyl rings and the tetrabutylammonium cations prevented the structural analysis from being completed (R = 0.0554, Rw = 0.1536, see Supporting Information). Other attempts of recrystallization from other solvents or with other phosphines are in progress. However, even if they are not definitive, the Ru−N and N−P bond lengths of 1.923(16) and 1.499(18) Å (average value), respectively, and the RuNP bond angle of 138.1(11)° (average value) are reliable and fall within the range of reported values for related osmium complexes.[57,58] To the best of our knowledge,

(54) Fan, L.; Xu, L.; Gao, G.; Li, F.; Li, Z.; Qiu, Y. *Inorg. Chem. Commun.* **2006**, *9*, 1308−1311.
(55) Sadakane, M.; Tsukuma, D.; Dickman, M. H.; Bassil, B.; Kortz, U.; Higashijima, M.; Ueda, W. *Dalton Trans*. **2006**, 4271−4276.
(56) Eikey, R. A.; Abu-Omar, M.-M. *Coord. Chem. Rev.* **2003**, *243*, 83−124.
(57) Demadis, K. D.; Bakir, M.; Klesczewski, B. G.; Williams, D. S.; White, P. S.; Meyer, T. J. *Inorg. Chim. Acta* **1998**, *270*, 511−526.

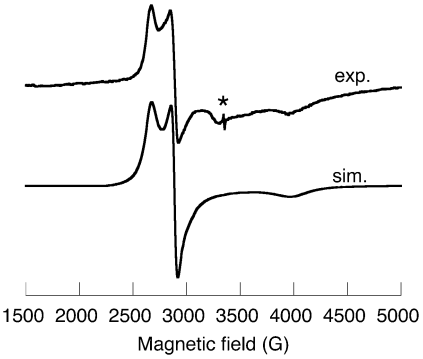

Figure 8. Solid-state EPR spectrum of solid $TBA_3[PW_{11}O_{39}\{Ru^{V}NPPh_3\}]$ (**2**) at 100K (*: impurity in the cavity).

compound **2** is indeed the first ruthenium-phosphoraniminato derivative formed by phosphine reduction of a ruthenium(VI)-nitrido species to be structurally characterized. According to the number of tetrabutylammonium cations around the polyanion, the Ru center should be assigned a +V, rather than the expected +IV, oxidation sate. Although most of nitrido-osmium-(VI) complexes are reduced by phosphines to give osmium-(IV)-phosphoraniminato derivatives, $[Os^{VI}N(DBCat)_2]^-$ (DBCat : 3,5-di-*tert*-butylcatecholate) unusually reacts with triphenylphosphine to yield $[Os^{V}(NPPh_3)(DBCat)_2]$.[58] Spontaneous oxidation in the presence of a POM is also precedented: for example, we have shown that the reaction between $[Re^{V}NCl_2(PPh_3)_3]$ and $[H_2PW_{11}O_{39}]^{5-}$ yields $[PW_{11}O_{39}\{Re^{VI}N\}]^{4-}$.[30,59] Since the relatively narrow signal observed in the ^{31}P NMR spectrum of **2** ($\Delta\nu_{1/2} = 90$ Hz) shows no narrowing during ^{1}H decoupling, it was attributed to the polyoxometalate core, while the signal of the phosphoraniminato phosphorus is probably too broad to be observed, because of the vicinity of the paramagnetic ruthenium center.

The X-band EPR spectrum of **2**, recorded in the solid state at 100 K, is represented in Figure 8 (up). This spectrum shows features at $g_1 = 2.51$, $g_2 = 2.32$, and $g_3 = 1.68$. It is in agreement with a rhombic $S = 1/2$ spin system (see simulation Figure 8, down). The large *g*-anisotropy clearly indicates that the spin density is mainly metal-centered and thus supports a +V oxidation state for the ruthenium (d^3 low spin). This is, to our knowledge, the first example of a Ru^{V}-phosphoraniminato EPR spectrum. Furthermore, there are few examples of EPR spectra of Ru^{V} complexes in the literature.[60−63] Among these, the two structurally characterized[61,64] species are pentacoordinated Ru=O complexes with low *g* anisotropy (for example $g_1 = 2.08$, $g_2 = 1.98$ and $g_3 = 1.91$).[61] In those cases, the low *g*-anisotropy indicates that the electronic ground state is well removed from excited states, consistent with the observed distorted trigonal bipyramidal geometry, resulting only in second-order contribution of the spin-orbit coupling to the *g*-matrix. On the contrary, in our case, the large *g*-anisotropy is indicative of strong spin−orbit interactions. This is in agreement with the pseudo C_{4v} geometry deduced from the preliminary X-ray study. Indeed, in such a geometry, the near degeneracy of the d_{xz} and d_{yz} orbitals should lead to two nearly degenerated ground states and in turn to first-order perturbation of the *g*-tensor by the spin-orbit coupling, a well-known effect in low spin Fe^{III} species,[65] resulting in large *g*-anisotropy.

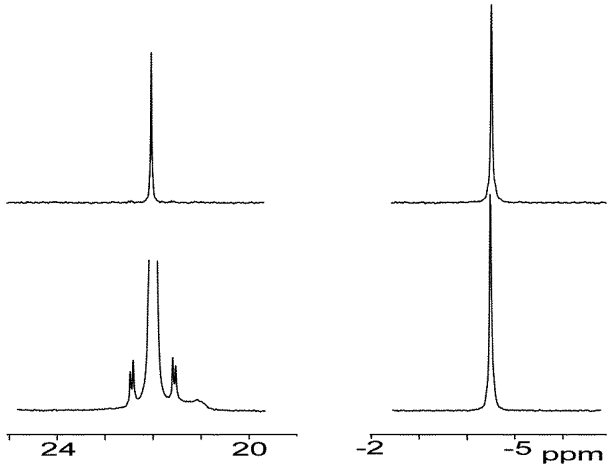

Figure 9. Evidence for the release of $[Ph_3P{=}N{=}PPh_3]^+$ at 22 ppm : top ^{31}P NMR spectrum of a solution of $TBA_4[PW_{11}O_{39}\{Ru^{VI}N\}]$ (**TBA-1**) in CH_3CN/CD_3CN (3:1) in the presence of 4 equiv of triphenylphosphine; bottom after addition of an authentic sample of $[Ph_3P{=}N{=}PPh_3]Cl$.

Further additions of phosphine result in the subsequent formation of several species (see Figure 7). Among the final products $[PW_{11}O_{39}Ru^{III}(NCCH_3)]^{4-}$ (−70 ppm, $\Delta\nu_{1/2} = 1000$ Hz)[17] is identified by ^{31}P NMR as well as the bis(triphenylphosphane)iminium cation ($[Ph_3P{=}N{=}PPh_3]^+ = PPN^+$) (22 ppm, $\Delta\nu_{1/2} = 0.7$ Hz). The latter was identified by adding a small amount of an authentic sample of PPNCl in the NMR tube and checking that the only effect was the increase of the intensity of the signal at 22 ppm, with no new signal appearing (see Figure 9). According to ^{31}P NMR spectroscopy, the amount of PPN^+ produced by addition of 3 equiv of PPh_3 is nearly twice that of starting **1**. This in turn suggests that the signals at 195 and −415 ppm correspond to species without nitrogenous ligands. Formation of the iminium, although not reported until now (to our knowledge) from ruthenium-nitrido complexes, is not without precedent for osmium derivatives: $[Os^{IV}(tpy)Cl_2(NPPh_3)]^+$ (tpy = terpyridine) was shown to release PPN^+ through the reaction with an excess of phosphine.[57] Although the reactivity of ruthenium-nitrido complexes toward phosphine has already been addressed in the literature, little is described about the characterization of the products, the characterization of ruthenium-phosphoraniminato relying only on IR and ^{31}P NMR spectroscopy. This is at variance with the chemistry of osmium-nitrido complexes, which has been extensively studied in the group of T. J. Meyer.[66] In one case, the ruthenium-phosphoraniminato derivative has been reported to evolve upon standing with release of the free phosphinimine Ph_3PNH.[36] In our case no Ph_3PNH could be detected (^{31}P NMR signal at 22.6 ppm, according to a freshly prepared authentic sample). Forma-

(58) Fang, G.-S.; Huang, J.-S.; Zhu, N.; Che, C.-M. *Eur. J. Inorg. Chem.* **2004**, 1341−1348.
(59) Following a question from one of the reviewers, we can exclude the concomitant reduction of the polyanion, on the basis of optical features: one-electron-reduced polyoxotungstates are deep blue because of the intervalence charge transfer W(V)−W(VI) (see for example, Livage, J.; Launay, J.-P. *et al. J. Am. Chem. Soc.* **1983**, *105*, 6817−6823), at variance with compound **2**, which is orange with an electronic absorption at 442 nm ($\log \epsilon = 3.7$, see Experimental Section).
(60) Neumann, R.; Abu-Gnim, C. *J. Am. Chem. Soc.* **1990**, *112*, 6025−6031.
(61) Dengel, A. C.; Griffith, W. P.; O'Mahoney, C. A.; Williams, D. J. *J. Chem. Soc., Chem. Commun.* **1989**, 1720−1721.
(62) Dengel, A. C.; Griffith, W. P. *Inorg. Chem.* **1991**, *30*, 869−871.
(63) Kuan, S. L.; Tay, E. P. L.; Leong, W. K.; Goh, L. Y.; Lin, C. Y.; Gill, P. M. W.; Webster, R. D. *Organometallics* **2006**, 6134−6141.
(64) Fackler, N. P. L.; Zhang, S.; O'Halloran, T. V. *J. Am. Chem. Soc.* **1996**, *118*, 481−482.
(65) Taylor, C. P. S. *Biochim. Biophys. Acta* **1977**, *491*, 137−149.
(66) Meyer, T. J.; Huynh, M. H. V. *Inorg. Chem.* **2003**, *42*, 8140−8160.

tion of Ru(III) complexes in the presence of an excess of phosphine is also precedented.[67] Identification of the different species and their thorough characterization together with their interplay are under current investigation and will be reported in a subsequent paper.

Summary and Conclusion

In this paper, we describe a very simple method for the synthesis of the ruthenium-nitrido derivative $[PW_{11}O_{39}\{Ru^{VI}N\}]^{4-}$ (**1**), which can be obtained either as an alkaline cation salt (Cs or Rb) or as a tetrabutylammonium salt. In this compound, the oxidation state of the Ru cation has been proved to be +VI by XAS and NMR spectroscopy. Furthermore, we have also demonstrated for the first time that a metal-nitrido function could still be reactive after its incorporation into a polyoxometalate core. Indeed, **TBA-1** reacts with triphenylphosphine to generate the first ruthenium-phosphiniminato derivative of a polyoxometalate: $[PW_{11}O_{39}\{RuNPPh_3\}]^{3-}$. In the course of the reaction of **1** with PPh_3 the bis(triphenylphosphane)iminium cation $[Ph_3P{=}N{=}PPh_3]^+$ is ultimately released. Much is still to be understood in the reactivity of **TBA-1** with PPh_3 or other phosphines and it is under investigation.

The cleavage of the ruthenium−nitrogen bond and the formation of PPN^+ validate the potential use of nitrido derivatives of polyoxometalates in nitrogen-atom transfer reactions, a type of reaction still under active investigations.[68] Albeit interesting from a mechanistical point of view, phosphines are probably not the most synthetically attractive substrate for this transfer. Our goal will now be to transfer this reactivity to other nucleophilic substrates, such as carbanions or enriched alkenes.

Experimental Section

Instrumentation and Techniques of Measurement. IR spectra were recorded from KBr pellets, on a Bio-Rad Win-IR FTS 165 FT-IR spectrophotometer. UV−visible spectra were recorded on a Shimadzu UV-2101 spectrophotometer. The ^{31}P (121.5 MHz) NMR spectra were obtained at room temperature in 5 mm o.d. tubes on a Bruker AvanceII 300 spectrometer equipped with a QNP probehead. The chemical shifts are given according to IUPAC convention with respect to 85% H_3PO_4 and were measured by the substitution method. ^{183}W NMR spectra were recorded in 10 mm o.d. tubes on the Bruker AvanceII 300 spectrometer operating at 12.5 MHz; the ^{31}P decoupling spectra were obtained by using a triple resonance low-frequency probehead with a ^{31}P decoupling coil. ^{183}W chemical shifts were measured with respect to 2 M Na_2WO_4 solution in alkaline D_2O by using saturated $H_4[SiW_{12}O_{40}]$ as a secondary external standard ($\delta = -103.8$ ppm).[69] XANES (X-ray absorption near-edge structure) and EXAFS (extended X-ray absorption fine structure) data were obtained on a synchrotron source at ELETTRA (Trieste, Italy) on the XAFS beamline equipped with a Si(311) double monochromator. The spectra were recorded at the ruthenium-K edge (22 117 eV) in transmission mode. The samples were ground and homogeneously dispersed in cellulose pellets, except for $[(salchda)Ru^{VI}N](ClO_4)$ which was carefully ground and dispersed on a kapton tape. The experiment was calibrated with a Ru metal foil. After background correction, the XANES spectra were normalized at the end of the energy range. The EXAFS analysis was performed by using the standard procedure "EXAFS pour le MAC" package.[70] The EXAFS signal was extracted from the data by subtracting a linear preedge background and normalized by the Lengeler−Eisenberger procedure.[71] The pseudo-radial distribution function was given by the Fourier transform (FT) of $\omega(k)k^3\chi(k)$, where $\omega(k)$ is a Kaiser−Bessel window with a smoothness parameter equal to 3. The k limits are equal to 3−14 $Å^{-1}$. Single-scattering fits of experimental curves were performed with the RoundMidnight program[72] with *ab initio* amplitude and phase functions calculated using FEFF7 code[73] from $[(salchda)Ru^{VI}N](ClO_4)$ for the RuN fragment and from $Cs_5[PW_{11}O_{39}\{Ru^{II}(H_2O)(p\text{-cymene})\}]$[34] for the POM fragment. X-band EPR spectra were recorded on a Bruker ELEXSYS 500 X-band spectrometer. For low-temperature studies, an Oxford Instrument continuous flow liquid cryostat and a temperature control (ITC 503) system were used. The temperatures have been calibrated using a RhFe thermoresistance that was put inside a 5-mm quartz tube. All the simulations were performed using the XSophe software (4.0 version) developed by the department of Mathematics at the University of Queensland, Brisbane, Australia, and obtained from Brüker Analytik GmbH, Rheinstetten, Germany.

Synthesis. The reagents $K_7[PW_{11}O_{39}]\cdot 14H_2O$,[74] $Cs_2[Ru^{VI}NCl_5]$, and $TBA[Ru^{VI}NCl_4]$[40] were synthesized according to the published procedures, as well as $[(salchda)Ru^{VI}N](ClO_4)$ (salchda = *N*,*N*′-bis(salicylidene)*o*-cyclohexyldiamine dianion),[32] and their purity was confirmed by infrared spectroscopy, ^{31}P NMR for $K_7[PW_{11}O_{39}]$, and ^1H NMR for $[(salchda)Ru^{VI}N](ClO_4)$. *Warning: perchlorate salts are potentially explosive! Great care should be used in handling.* Reagent grade solvents (acetonitrile, diethyl ether, dichloromethane, etc.), reagents (PPh_3), and reference compounds ($[Ru(acac)_3]$ (acac = acetylacetonate), RuO_2) were purchased from Aldrich, ACROS Organics, or Strem Chemicals and used as received. Chemical analyses were performed by the Service de Microanalyses (Université Pierre et Marie Curie, Paris, France) and the Laboratoire Central d'Analyses du CNRS (Vernaison, France).

$Cs_4[PW_{11}O_{39}\{Ru^{VI}N\}]$ (Cs-1). After dissolution of $K_7[PW_{11}O_{39}]\cdot 14H_2O$ (0.74 g, 0.25 mmol) in 10 mL of distilled water, an aqueous solution (5 mL) of $Cs_2[Ru^{VI}NCl_5]$ (0.14 g, 0.25 mmol) was added under stirring at room temperature. An almost immediate greyish precipitate formed. The reaction mixture was stirred for 30 min at room temperature and then filtered on a fritted glass funnel. $Cs_4[PW_{11}O_{39}\{Ru^{VI}N\}]$ was obtained as a greyish-green solid in 48% yield. IR (KBr) ν_{max} (cm^{-1}): 334 (w), 389 (s), 519 (m), 750 (sh), 810 (s), 883 (s), 979 (s), 1072 (s), 1093 (sh). MAS ^{31}P RMN (162.0 MHz, 300 K) δ (ppm): −14.5 ppm

$TBA_4[PW_{11}O_{39}\{Ru^{VI}N\}]$ (TBA-1). A solution of $K_7[PW_{11}O_{39}]\cdot 14H_2O$ (6.434 g, 2.0 mmol in 10 mL of water) was added dropwise over 5 min in a gently stirred solution of $TBA[Ru^{VI}NCl_4]$ (1.000 g, 2.0 mmol in 12.5 mL of acetonitrile). A brown suspension formed immediately. The reaction mixture was stirred at room temperature for an additional 10 min. Filtration of the solution yielded a green solid that was washed with 2 mL of a 50:50 mixture of acetonitrile and water and then 3 mL of water. The solid was redissolved in acetonitrile (28 mL), leaving a white residue (identified by infrared and ^{31}P NMR as $TBA_3[PW_{12}O_{40}]$) that was filtered off. Upon slow evaporation of the solution in a covered beaker sitting in a water bath, green crystals of $TBA_4[PW_{11}O_{39}\{RuN\}]$ deposited after 3 days (600 mg, 32% calculated from the limiting TBA). The codeposition of white crystals of $TBA_3[PW_{12}O_{40}]$ is sometimes observed. Anal. Calcd for $C_{64}H_{144}N_5PW_{11}RuO_{39}$: C, 20.43; H, 3.86; N, 1.86; P, 0.82; W, 53.75; Ru, 2.68. Found: C, 20.15; H, 3.74; N, 1.69; P, 0.84; W, 52.35; Ru, 3.04. IR (KBr) ν_{max} (cm^{-1}): 333 (w), 376 (m), 389 (s), 504 (m), 518 (m), 596 (w), 750 (sh), 810 (s), 889 (s), 913 (s), 962 (s), 1013 (sh), 1028 (w), 1072 (s), 1093 (sh), 1107 (w), 1153 (w), 1382 (w), 1484 (m), 2875 (m), 2937 (sh), 2962 (s). UV−vis (CH_3-

(67) Yip, K.-L.; Yu, W.-Y.; Chan, P.-M.; Zhu, N.-Y.; Che, C.-M. *Dalton Trans.* **2003**, 3556−3566.
(68) Mendiratta, A.; Cummins, C. C.; Kryatova, O. P.; Rybak-Akimova, E. V.; McDonough, J. E.; Hoff, C. D. *J. Am. Chem. Soc.* **2006**, *128*, 4881−4891.
(69) Acerete, R.; Hammer, C. F.; Baker, L. C. W. *J. Am. Chem. Soc.* **1979**, *101*, 267−269.
(70) Michalowitcz, A. EXAFS version 1998 for Mac OS9, http://www.univ-paris12.fr/40615508/0/fiche_3000A__pagelibre/.
(71) Lengeler, B.; Eisenberg, P. *Phys. Rev. B* **1980**, *21*, 4507.
(72) Michalowitcz, A. RoundMidnight, http://www.univ-paris12.fr/40615508/0/fiche_3000A_pagelibre/.
(73) Zabinsky, S. I.; Rehr, J. J.; Ankudinov, J. J.; Albers, R. C.; Eller, M. J. *Phys. Rev. B* **1995**, *52*, 2995−3009.
(74) Souchay, P. *Polyanions et polycations*; Gauthier-Villars: Paris, 1963.

CN) λ_{max}, nm (log ϵ): 605 (1.5), 380 (sh, 2.7). ^{31}P NMR (121.5 MHz, CD_3CN, 300 K) δ (ppm): −13.8 ($\Delta\nu_{1/2}$ = 1 Hz). ^{183}W NMR (12.5 MHz, CH_3CN/CD_3CN, 300K) δ (ppm): −87.3, −90.8, −96.4, −104.7, −133.2, −133.9. (12.5 MHz, DMF/d_6-acetone, 262 K) δ (ppm): −86.9 (2W), −91.0 (2W), −95.7 (1W), −104.1 (2W), −133.0 (2W),−134.4 (2W). Crystallographic data: cubic, space group: *I*43*m*, a = 17.755-(2) Å, V = 5597(2) Å^{-3}.

Monitoring of the Reaction of TBA-1 with Triphenylphosphine. In a 5 mm NMR tube were introduced 0.3 mL of a solution of TBA_4-$[PW_{11}O_{39}\{RuN\}]$ (263 mg in 5 mL of acetonitrile) and 0.1 mL of CD_3-CN. A control NMR spectrum indicated the presence of about 25**%** $[PW_{11}O_{39}]^{7-}$ and traces of $[PW_{12}O_{40}]^{3-}$. In the NMR tube, 3.48 μL of a solution of triphenylphosphine (474 mg in 20 mL CH_3CN**)** (0.1 equiv vs $TBA_4[PW_{11}O_{39}\{Ru^{VI}N\}]$ calculated from the first spectrum) was then added via an Eppendorf pipet. The solution was quickly homogenized, and two NMR spectra were then recorded (600/−500 ppm and 60/−40 ppm**).** This process took between 15 and 20 min and was repeated until 3 equiv of triphenylphosphine had been added.

Isolation of $TBA_3[PW_{11}O_{39}\{RuNPPh_3\}]$ (2). Triphenylphosphine (1 mL of a 0.067 mol L^{-1} acetonitrile solution, 0.5 equiv vs TBA_4-$[PW_{11}O_{39}\{Ru^{VI}N\}]$) was slowly added to a solution of $TBA_4[PW_{11}O_{39}$-$\{Ru^{VI}N\}]$ (505 mg, 0.13 mmol dissolved in 15 mL acetonitrile). The green solution turned red. The brown solid formed by addition of 40 mL of diethyl ether was separated by centrifugation, redissolved in a minimum of 1:1 mixture of acetonitrile and dichloromethane. Elution over a silica column (silica gel 60, 0.063−0.200 mm, eluant CH_2Cl_2/CH_3CN 1:1) separated two fractions, the first one orange and the second one green (unreacted $TBA_4[PW_{11}O_{39}\{RuN\}]$). The first fraction was concentrated to dryness by rotatory evaporation at room temperature, yielding 0.118 g (48% relative to PPh_3) of **2** as a red-orange powder. Slow diffusion of diethyl ether in a 6 mM acetonitrile solution yielded the red crystals of **2** used for the X-ray diffraction study. IR (KBr) ν_{max} (cm^{-1}): 388 (s), 518 (m), 690 (w), 724 (w), 806 (vs), 886 (s), 969 (s), 1049 (m), 1087 (s), 1114 (w), 1381 (w), 1438 (w), 1484 (m), 2874 (w), 2833 (w), 2962 (m). UV (CH_3CN) λ_{max}, nm (log ϵ): 442 (3.7). ^{31}P RMN (121.5 MHz, CD_3CN, 300 K) δ (ppm): 322 ($\Delta\nu_{1/2}$ = 90 Hz). ^{1}H NMR (300.13 MHz, CD_3CN, 300 K) δ (ppm): 1.00 (t, 36H, ($CH_3(CH_2)_3)_4N^+$), 1.41 (h, 24H, ($CH_3CH_2(CH_2)_2)_4N^+$), 1.67 (m, 24H, ($CH_3CH_2CH_2CH_2)_4N^+$), 3.16 (m, 24H, ($CH_3(CH_2)_2CH_2)_4N^+$), 7.57 (t, J = 7.0 Hz, 3H, *p*-C_6H_5), 9.44 (d, J = 5.6 Hz, 6H, *m*-C_6H_5), 12.05 (s, $\Delta\nu_{1/2}$ = 25 Hz, 6H, *o*-C_6H_5).

Acknowledgment. We acknowledge Dr. Guillaume Blain for the access to the Elexsys EPR spectrometer of the Institut de Chimie Moléculaire et des Matériaux d'Orsay, UMR CNRS 8182, Université Paris-Sud, Patricia Beaunier for the EDX study, Séverine Renaudineau for the preparation of the precursors, and Dr. Christophe Cartier-dit-Moulin for fruitful discussions on the XAS. We are especially grateful to Prof. Pierre Gouzerh for his continuous interest to this work as well as for his valuable advice. The help in carrying out the XAS study provided by the ELETTRA staff is gratefully acknowledged. This work was supported by the CNRS, the Université Pierre et Marie Curie, and by the EEC, for funding the XAS study at ELETTRA.

Supporting Information Available: EDX spectrum of Cs_4-$[PW_{11}O_{39}\{Ru^{VI}N\}]$ and $Cs_5[PW_{11}O_{39}\{Ru(p\text{-cymene})(H_2O)\}]$; IR and ^{31}P MAS spectra of $Cs_4[PW_{11}O_{39}\{Ru^{VI}N\}]$ and IR spectrum of $TBA_4[PW_{11}O_{39}\{Ru^{VI}N\}]$; theoretical matrix connectivity for $[\alpha\text{-}PW_{11}O_{39}\{ML\}]^{n-}$ and full assignment of the ^{183}W NMR spectrum of $TBA_4[PW_{11}O_{39}\{Ru^{VI}N\}]$; Ru-K edge XANES spectra of $Cs_4[PW_{11}O_{39}\{Ru^{VI}N\}]$ and $TBA_4[PW_{11}O_{39}$-$\{Ru^{VI}N\}]$; modulus and imaginary part of the Fourier transform of $TBA_4[PW_{11}O_{39}\{Ru^{VI}N\}]$ filtered between 1 and 2.5 Å; IR, ^{1}H, and ^{31}P NMR spectra of $TBA_4[PW_{11}O_{39}\{Ru^{V}NPPh_3\}]$ and single-crystal X-ray analysis. Evolution of the ^{31}P NMR spectrum (Expanded part +30 −15 ppm) of $TBA_4[PW_{11}O_{39}$-$\{Ru^{VI}N\}$ in the presence of increasing amounts of PPh_3. This material is available free of charge via the Internet at http://pubs.acs.org.

JA071137T